Journal of Electronic Research and Application, 2026, Volume 10, Issue 2
http://ojs.bbwpublisher.com/index.php/JERA
ISSN Online: 2208-3510
ISSN Print: 2208-3502

A Dual-Adaptive Electronic Monitoring System for Robust State-of-Charge Estimation of *LiFePO₄* Batteries in High-Precision Applications

Chaomin Yue[1]*, Yongpeng Zheng[1], Zhicheng Zhu[1,2]

[1]College of Mechanical Engineering, University of Shanghai for Science and Technology, Shanghai 200093, China
[2]School of Automotive Engineering, Jiangxi Polytechnic University, Jiujiang 332007, Jiangxi, China

**Corresponding author: Chaomin Yue, yuemin261@gmail.com*

Abstract: Electronic battery management systems (BMS) require high-precision state-of-charge (SOC) estimation to ensure the reliability of integrated electronic applications. However, the flat voltage plateau of $LiFePO_4$ batteries poses a significant challenge for electronic sensing and state observation. This paper proposes a synergistic dual-adaptive framework designed for real-time electronic monitoring. The framework integrates a thermodynamic-gradient gain-re-allocation (TG-GRA) mechanism into the recursive least squares algorithm to enhance parameter identification fidelity. Furthermore, a current-adaptive augmented extended Kalman filter (CAEKF) is developed to optimize the electronic control loop by dynamically adjusting noise covariance and compensating for voltage hysteresis. Experimental validation across 32 dynamic cycles demonstrates that the proposed electronic sensing strategy reduces the root-mean-square error (RMSE) to 1.3%. With its low computational overhead, this framework provides a robust and efficient system-level solution for embedded electronic research and applications.

Keywords: SOC estimation; $LiFePO_4$ battery; Electronic monitoring systems; Adaptive filtering

Online publication: March 31, 2026

1. Introduction

As primary power sources for automated systems like AGVs, $LiFePO_4$ batteries require precise electronic monitoring via the BMS to ensure operational safety [1–4]. To address the poor SOC observability in the OCV plateau, existing approaches can be broadly categorized into three paradigms as follows:

(i) Enhanced physics-based observers [5–8];
(ii) Data-driven black-box models [8–13];
(iii) Active excitation-based feature extraction [14].

However, the flat OCV-SOC plateau in LFP batteries compromises the observability of state observers, leading to estimation drift in high-frequency manufacturing. To address this without intrusive calibration, this study proposes a dual-adaptive framework. We embed a TG-GRA mechanism into the RLS algorithm for physically consistent parameter updates and employ a CAEKF with current-magnitude-dependent noise tuning to ensure robust monitoring with minimal computational cost.

2. Experimental setup and design of experiments

This section details the experimental platform, test protocols, and data collection procedures. A schematic of the battery test system is shown in **Figure 1**, and the specifications of the test cells are summarized in **Table 1**. All experiments were conducted under controlled thermal conditions: the cell was placed in a temperature chamber maintained at 25 ± 1 ∘ C and cycled using a Neware NEBULA-NEEFLCTO-5300 battery cycler. Two sets of experiments were performed as shown in **Figure 2**.

Table 1. Basic performance parameters of battery

Item	Specification
Cathode/anode materials	C
Nominal capacity	280Ah
Nominal voltage	3.2V
Standard charge/discharge current	Charge: 0.5C; Discharge: 0.5C
Charge/discharge cut-off voltages	Charge cut-off: 3.65 V ; Discharge cut-off: 2.5 V
Operating temperature range	Charge: 0°C to 55°C; Discharge:–20°Cto 55°C

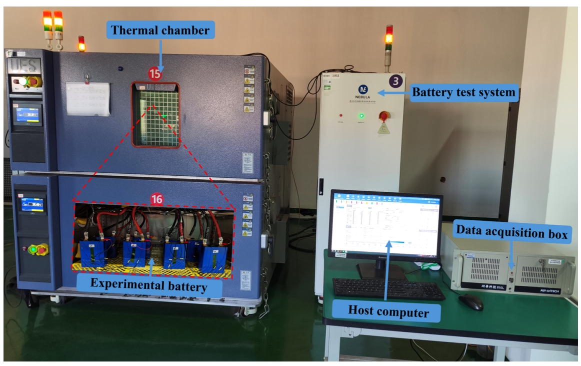

Figure 1. Layout and equipment connection diagram of battery test platform.

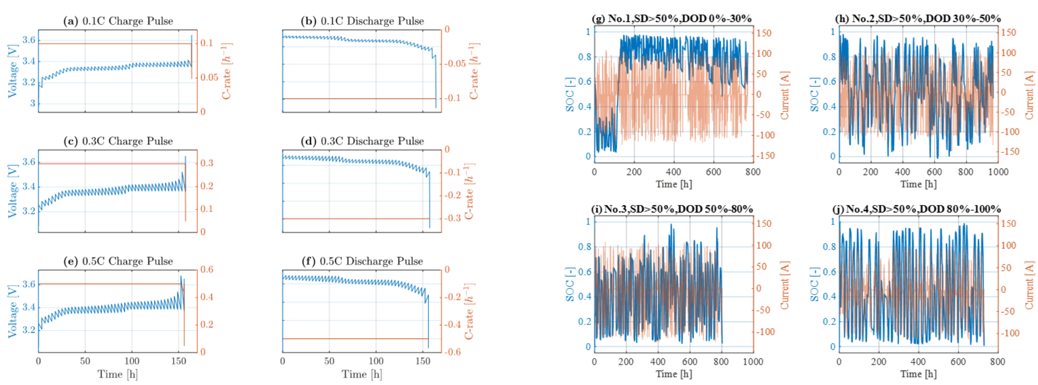

Figure 2. Measured voltage and C-rate profiles during GITT tests at different rates (a)–(f). SOC profiles and corresponding dynamic current excitations for four representative test cases: correspond to cell 1 to cell 4 (g)–(j).

3. Methodology

The proposed framework (**Figure 3**) integrates identification and filtering layers for joint adaptation. The TG-GRA mechanism reallocates update gains based on local OCV-SOC sensitivity, ensuring parameter consistency across the full SOC range. At the filtering layer, the CAEKF introduces current-dependent noise scaling to balance model trust and measurement correction, alongside a rate-dependent hysteresis model to isolate polarization artifacts. This adaptation-prediction-correction paradigm is optimized for low-overhead embedded deployment (**Figure 4**).

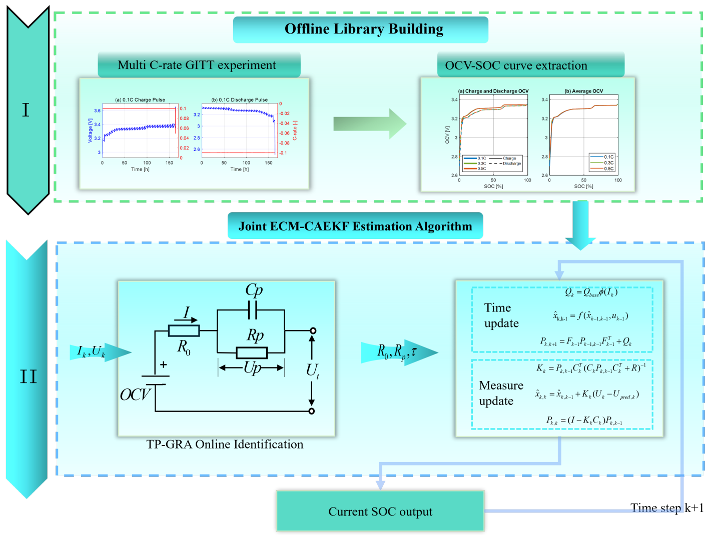

Figure 3. Overall architecture of the state-of-charge estimation system integrating TG-GRA and CAEKF.

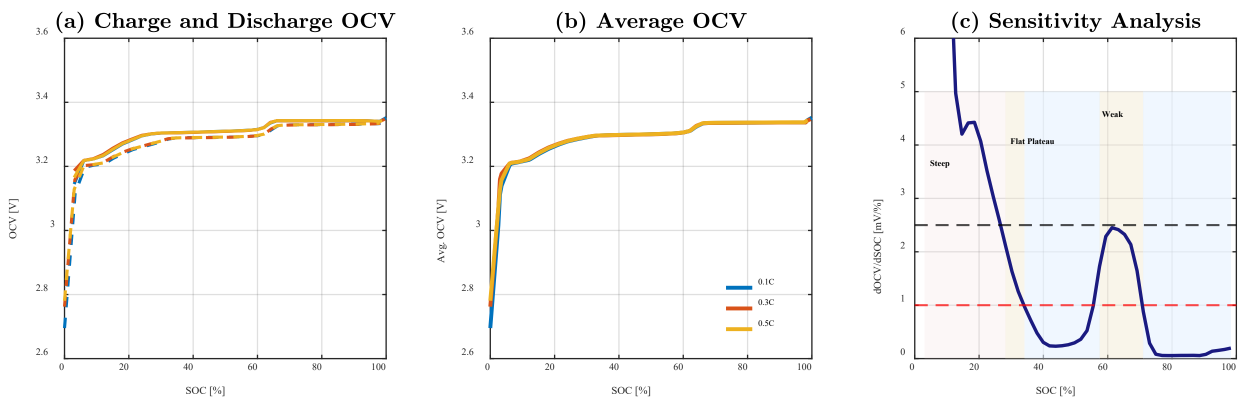

Figure 4. (a) OCV versus SOC measured after GITT pulses at 0.1C, 0.3C, and 0.5C rates (b) Rate-averaged OCV-SOC curve obtained by aligning and averaging the data from all tested C-rates (c) dOCV/dSOC characteristics of the test cell.

3.1. Model parameter identification under the TG-GRA mechanism

To mitigate attribution bias in OCV-sensitive regions, the FFRLS algorithm is augmented with a gain redistribution mechanism driven by the local thermodynamic gradient. Traditional methods employing offline lookup tables or fixed-gain recursive algorithms often fail to decouple thermodynamic voltage drift from dynamic polarization responses, particularly in the non-plateau regions of $LiFePO_4$ batteries, leading to parameter attribution bias. To address this, the proposed TG-GRA mechanism does not apply uniform weight updates to the parameter vector.

Instead, it dynamically senses the strength of the thermodynamic gradient and constructs an asymmetric gain adjustment matrix. In OCV-sensitive intervals, it prioritizes the correction of thermodynamic-related weights while suppressing the update step size of polarization parameters (including ohmic resistance, polarization resistance, and time constant). This gradient-induced gain steering ensures high physical fidelity of model parameters under varying operating conditions, partially overcoming the model-state coupling issue that causes model mismatch.

3.2. Current-adaptive hysteresis modeling and extended Kalman filtering

Compared to conventional EKF approaches, the proposed framework enhances the filtering layer along three dimensions: model decoupling, physics-informed compensation, and dynamic regulation of stochastic uncertainties. The framework improves the EKF in three ways. First, it decouples the model by updating state matrices through TG-GRA while sourcing OCV from an offline lookup table. This ensures the innovation signal exclusively reflects Coulomb-counting drift, enabling robust closed-loop correction. Second, it employs a current-adaptive hysteresis model to isolate polarization artifacts that low-order ECMs often neglect. Unlike conventional models, this approach captures current-dependent saturation rates. The evolution of hysteresis state h is defined by:

$$\frac{dh}{dt} = \kappa|I(t)| \cdot [H_{lim}(I, SOC) - h(t)] \tag{1}$$

Furthermore, to account for the non-stationary nature of modeling errors and stochastic disturbances under complex C-rate profiles, the algorithm incorporates a current-adaptive noise regulation mechanism. Recognizing that large current pulses significantly amplify linearization errors, an adaptive scaling factor is introduced. During recursive updates, this factor dynamically adjusts the process noise covariance Q in proportion to the instantaneous current magnitude, thereby achieving a real-time balance between trust in model prediction and reliance on measurement feedback. Under high-C-rate conditions, the algorithm increases Q to reduce dependence on the model's internal dynamics and enhance correction from terminal voltage measurements, thus ensuring global robustness across the full operational dynamic range.

4. Results and discussion

4.1. Model identification accuracy

The proposed TG-GRA mechanism effectively resolves the parameter identification mismatch resulting from thermodynamic gradient disparities in LFP batteries. In typical test cycles, by employing a gain redistribution strategy to regulate parameter update directions, the method maintains parameter proximity to physical reality despite thermodynamic variations. This leads to a terminal voltage RMSE reduction from 32.22 mV to 17.47 mV compared to the standard FFRLS. Comprehensive validation confirms a 35.9% average RMSE improvement across all test cases (**Figure 5**).

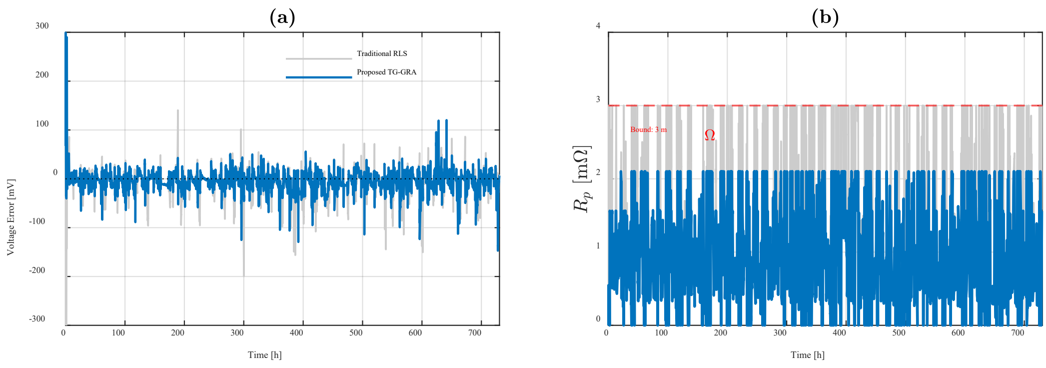

Figure 5. (a) Comparison of voltage prediction error (b) Identified polarization resistance R_p comparison.

4.2. SOC estimation under dynamic cycles

To verify the generalizability of the proposed AEKF-GRA algorithm, 32 sets of battery data with diverse cell characteristics and dynamic profiles were tested. **Figure 6** illustrates the distribution of SOC regions across these operating conditions. The experimental current was measured with a precision of 0.03%. To simulate real-world sensor inaccuracies, a constant +1% bias was added to the raw current, and a 30% initial positive offset was introduced to the SOC. The SOC calculated via ampere-hour integration using noise-free current serves as the reference. The error distribution for the 32 test cases is shown in **Figure 6**.

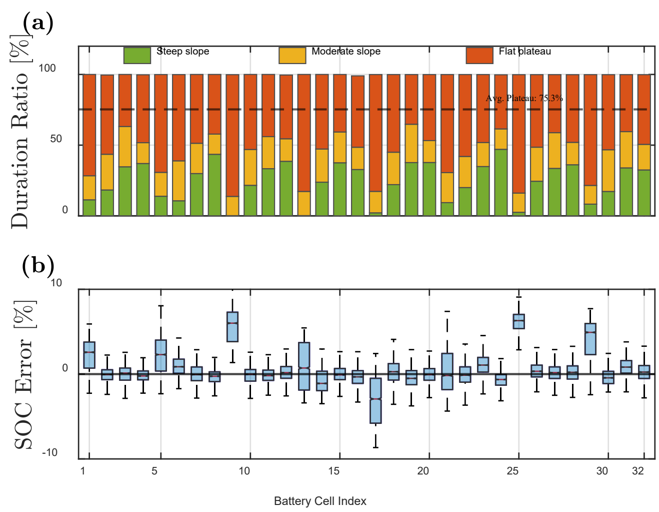

Figure 6. (a) Distribution of SOC dynamic regions across 32 cells (b) Statistical distribution of SOC estimation errors across 32 battery cells.

5. Conclusion

Accurate SOC estimation is vital for electronic monitoring systems. To overcome LFP observability limits, this study proposes a dual-adaptive framework. The TG-GRA mechanism ensures physical consistency in electronic circuit models during dynamic transitions. Conversely, the CAEKF provides robust measurement accuracy via adaptive noise tuning, reducing RMSE to 1.3%. This framework offers a high-performance electronic solution for optimized power electronics.

Disclosure statement

The author declares no conflict of interest.

References

[1] Barik S, Saravanan B, 2024, Recent Developments and Challenges in State-of-Charge Estimation Techniques for Electric Vehicle Batteries: A Review. Journal of Energy Storage, 2024(100).

[2] Demirci O, Taskin S, Schaltz E, et al., 2024, Review of Battery State Estimation Methods for Electric Vehicles: Part I: SOC Estimation. Journal of Energy Storage, 2024(87).

[3] Zhao T, Li W, Traversy M, et al., 2024, A Review on the Recycling of Spent Lithium Iron Phosphate Batteries. J Environ Manage, 2024(351): 119670.

[4] Zhou L, Lai X, Li B, et al., 2023, State Estimation Models of Lithium-Ion Batteries for Battery Management System: Status, Challenges, and Future Trends. Batteries, 9(2): 131.

[5] Lu C, Hu J, Zhai Y, et al., 2023, State of Charge Estimation Method Based on Linearization of Voltage Hysteresis Curve. Journal of Energy Storage, 72: 108481.

[6] Pei L, Wang T, Lu R, et al., 2014, Development of a Voltage Relaxation Model for Rapid Open-Circuit Voltage Prediction in Lithium-Ion Batteries. Journal of Power Sources, 2014(253): 412–418.

[7] Peng S, Zhang D, Dai G, et al., 2025, State of Charge Estimation for LiFePO4 Batteries Joint by PID Observer and Improved EKF in Various OCV Ranges. Applied Energy, 2025(377).

[8] Wei M, E M, Lian G, et al., 2024, Robust State of Charge Estimation of LiFePO4 Batteries Based on Sage_Husa Adaptive Kalman Filter and Dynamic Neural Network. Electrochimica Acta, 2024(477).

[9] Hossain Lipu M, Hannan M, Hussain A, et al., 2020, Data-Driven State of Charge Estimation of Lithium-Ion Batteries: Algorithms, Implementation Factors, Limitations and Future Trends. Journal of Cleaner Production, 2020(277).

[10] Jin Z, Fu S, Fan H, et al., 2025, Edge-Cloud Collaborative Method for State of Charge Estimation of Lithium-Ion Batteries by Combining Kalman Filter and Deep Learning. Energy, 2025(332): 137234.

[11] Tian J, Xiong R, Shen W, et al., 2021, State-of-Charge Estimation of LiFePO4 Batteries in Electric Vehicles: A Deep-Learning Enabled Approach. Applied Energy, 2021(291): 116812.

[12] Wang C, Li Z, Outbib R, et al., 2022, A Novel Long Short-Term Memory Networks-Based Data-Driven Prognostic Strategy for Proton Exchange Membrane Fuel Cells. International Journal of Hydrogen Energy, 47(18): 10395–10408.

[13] Wu X, Yan C, Wang L, et al., 2025, Data-Driven SOC Estimation Method for Power Batteries under Driving Cycle Conditions and a Wide Temperature Range. Energy, 2025(340): 139147.

[14] Gao Y, Onori S, 2025, Advancing SOC Estimation in LiFePO4 Batteries: Enhanced dQ/dV Curve and Short-Pulse Methods. eTransportation, 2025(26): 100466.